PAPER

Synthesis of well-defined α-fluorinated alkyl ester, ω-carboxyltelechelic polystyrenes and fabrication of their hydrophobic highly ordered porous films and microspheres†

Shuang-Shuang Zhang,[ab] Shao-Kui Cao,*[b] Su Wang,[b] Qiao-Ling Zhao,[a] Jian-Zhuang Chen,[a] Kun Cui[a] and Zhi Ma*[a]

Well-defined α-fluorinated alkyl ester, ω-carboxyl telechelic polystyrenes (PS) were synthesized via combining aminolysis of RAFT-polystyrene and thiol–ene "click" reaction simultaneously. The perfluoroalkyl end groups were $-CF_3$, $-(CF_2)_2-CF_3$ and $-(CF_2)_7-CF_3$, respectively. Highly ordered porous films of such telechelic PS with an average pore size about 1.00 μm were fabricated via a static breath-figure process. With the content of fluorine on the surface of porous films increasing from 1.04 wt%, to 1.64 wt% and 2.97 wt%, respectively, the water contact angle (WCA) of such porous films increased from 112° to 116° and 121° ± 0.4°, respectively, indicating their hydrophobicity. Interestingly, microspheres with average diameters of *ca.* 0.30–0.65 μm can be fabricated via a static BF process using methanol instead of water as the vapor atmosphere in the glass vessel.

Introduction

Benefitting from the presence of functional groups at the terminus of the chain, telechelic polymers (α,ω-functionality) have been widely used as precursors in the synthesis of block copolymers, cross-linking agents and compatibilizers in polymer blends.[1–3] Currently, a series of telechelic vinyl polymers with terminal hydroxyl, carboxyl, epoxy groups and carbon–carbon double bond have been prepared[4–8] by various methods, such as anionic polymerization,[9–12] atom transfer radical polymerization (ATRP),[6,13–16] reversible addition–fragmentation chain transfer (RAFT) polymerization,[4,17–23] and thiol–acrylate Michael reaction.[24] In addition, a facile one-pot strategy combining aminolysis with thiol–ene "click" reaction[25–29] showed high efficiency in the synthesis of diverse α,ω-telechelic polymers.

Due to the strong and highly polar C–F bond, fluorinated polymers have excellent physical and chemical properties such as low surface energy, low refractive index, high optical clarity, superior thermal and chemical resistance.[30–32] The fluorinated side chain aggregates at the air–polymer interface and the presence of the fluorine atom on the surface resulted in high hydrophobicity of the copolymer.[33–37] Because of their unique properties, fluoropolymers have attractive applications in automobile parts, protective clothing, electrical and electronic devices, optical as well as medical devices.[38,39] In the past decades, there have been several studies on the surface properties of polyfluoroacrylates and strategy for the synthesis of fluoropolymers have been reported. However, α,ω-perfluoro telechelic polymer was fewly reported. Ever before, Zhang *et al.* demonstrated well-defined α,ω-functional telechelic fluoropolystyrenes was gained via one-pot strategy combining aminolysis of RAFT-polystyrene and thiol–ene "click" reaction under incandescent-lamp irradiation.[29] Robinson *et al.* demonstrated a homologous series of α,ω-perfluorodicarboxylic acids was generated in a controlled free radical polymerization of tetrafluoroethylene using aqueous peroxydisulfate with either an iron or a copper promoter.[40] Mao *et al.* demonstrated a series of well-defined perfluoroalkyl end-functionalized poly(3-hexylthiophenes) were synthesized by Stille coupling of stannylated 2-perfluoroalkylthiophene with the bromine end of poly(3-hexylthiophenes). They found a negative correlation between perfluoroalkyl end groups lengths and device performance. Specifically, power conversion efficiency, short-circuit current density (J_{sc}), and maximum external quantum efficiency (EQE) systematically decreased with increasing perfluoroalkyl end-group length.[41]

Usually, porous films can be fabricated via a static breath-figure (BF) process in an aqueous vapor atmosphere.[42–51] Such highly ordered porous films can be applied in scaffold for cell growth,[52] size-selective seperation,[53] superhydrophobic

[a] Key Laboratory of Synthetic and Self-Assembly Chemistry for Organic Functional Molecules, Shanghai Institute of Organic Chemistry, Chinese Academy of Sciences, Shanghai, 200032, P. R. China. E-mail: mazhi728@sioc.ac.cn

[b] School of Materials and Engineering, Zhengzhou University, Zhengzhou, 450052, P. R. China. E-mail: caoshaokui@zzu.edu.cn

† Electronic supplementary information (ESI) available. See DOI: 10.1039/c5ra17073g

surfaces,[54,55] polymeric microsieves,[56] *etc.* However, when the water environment in the chamber was replaced with methanol, microspheres rather than porous films were observed.[57–59] The polymer microspheres were widely used in separation, catalysis carriers, drug delivery and so on directly or after surface functionalization.[57,59–62] Combined with the properties of fluoropolymer, in previous research work, the fabrication of porous films of fluorinated copolymer expanded the applicable fields by BF method.[63,64] Due to the introduction of fluorine element, the porous films obtained excellent hydrophobicity and chemical resistance. It is expected to be used in hydrophobic membrane, separation membrane and other fields of material for practical application.

From the above points of view, in this work, a series of α-fluorinated alkyl ester, ω-carboxyl telechelic PS (R–S–PS–COOH: R_1 = –(CH$_2$)$_2$–COO–CH$_2$–CF$_3$, R_2 = –(CH$_2$)$_2$–COO–CH$_2$–(CF$_2$)$_2$–CF$_3$, R_3 = –CH$_2$–CH(CH$_3$)–COO–(CH$_2$)$_2$–(CF$_2$)$_7$–CF$_3$) were synthesized *via* combining aminolysis of RAFT-polystyrene and thiol–ene "click" reaction under incandescent-lamp irradiation. Subsequently, porous films of α-fluorinated alkyl ester, ω-carboxyl-telechelic PS were fabricated *via* static BF process in an aqueous vapor atmosphere, and microspheres were fabricated *via* static BF process in methanol atmosphere. The morphology and hydrophobicity of such porous film and microspheres were preliminarily investigated by SEM, TEM and WCA determination, respectively.

Experimental

Materials

PS-CTA (M_n = 3200 g mol^{-1}, M_w/M_n = 1.08) was synthesized as previously reported using *S*-1-dodecyl-*S*′-(α,α′-dimethyl-α″-acetic acid)trithiocarbonate (DDMAT) as chain transfer agent in RAFT polymerization of styrene.[29] *n*-Hexylamine (*n*-HA, Aladdin, 99%), tri-*n*-butylphosphine (Bu$_3$P, Adamas, 98%+), 2,2-dimethoxy-2-phenylacetophenone (DMPA, Aladdin), 2,2,2-trifluoroethyl acrylate (TFEA) (J&K, 99%), 1*H*,1*H*-heptafluorobutyl acrylate (HFBA, J&K, 97%), 3,3,4,4,5,5,6,6,7,7,8,8,9,9,10,10,10-heptadecafluorodecyl methacrylate (HDFDM, Aldrich, 97%), tetrahydrofuran (THF) were refluxed over sodium/benzophenone and distilled under N$_2$ before use. All manipulations involving air- and/or moisture-sensitive compounds were carried out in a N$_2$-filled dry box or using Schlenk techniques.

Synthesis of α-fluorinated alkyl ester, ω-carboxyl telechelic PS *via* combining aminolysis of RAFT-polystyrene and thiol–ene "click" reaction simultaneously

The telechelic polymers **R$_1$–S–PS–COOH** and **R$_2$–S–PS–COOH** were synthesized as previously reported.[29] However, the **R$_3$–S–PS–COOH** with longer fluorinated chain end can not be synthesized in such procedure. Alternatively, a tandem strategy was employed as follows: **PS-CTA** (1.01 g, 0.32 mmol) was dissolved in 20 mL of anhydrous THF. The solution was purged with dry nitrogen for 15 min. 10-fold molar excess *n*-hexylamine, 5-fold molar excess tri-*n*-butylphosphine (Bu$_3$P) (5 equiv.
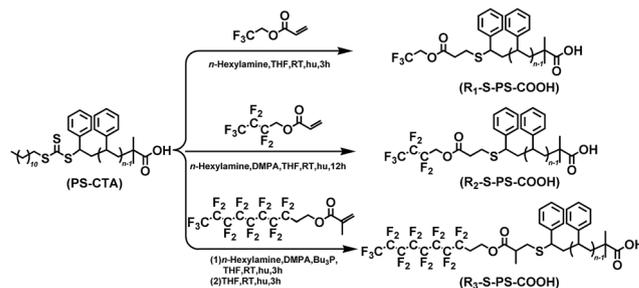
Scheme 1 Synthesis of α,ω-telechelic PS.

relative to thiol moiety) was successively added, then stirred for 3 h at room temperature to obtain HS–PS–COOH. After that, HS–PS–COOH (0.15 mmol, 1 equiv.), HDFDP (10 equiv.), photoinitiator (DMPA, 5 equiv.) in 10 mL of THF were introduced in a Schlenk flask and incandescent-lamp irradiated at room temperature (RT) for 3 h. The intensity of electric current was 25 A as measured by Xenon lamp XQ500W adjustable radiometer. The reaction mixture was precipitated in methanol (3 times), and then dried in a vacuum oven at room temperature for 24 h. The synthetic procedure was shown in Scheme 1. **R$_1$–S–PS–COOH:** $M_{n(GPC)}$ = 3400 g mol^{-1}, M_w/M_n = 1.05, ^{1}H NMR(CDCl$_3$): $\delta_{(ppm)}$ = 7.43–6.30 (m, H^d), 4.46–4.30 (m, H^l), 3.40–3.23 (m, H$^{e'}$), 2.50–1.35 (m, H$^{f+g+h+k+j}$), 1.33–1.20 (s, H$_2^i$), 1.06–0.82 (m, H$_1^i$). ^{19}F NMR (CDCl$_3$): $\delta_{(ppm)}$ = −73.67, −73.70, −73.72 ppm. ^{13}C NMR (CDCl$_3$): δ(ppm) = 147.86–143.30 (C^{K+P}), 133.76–120.73 (C^{L+R}), 50.51–36.52 (C$^{E+F+G+J}$), 28.20–24.14 (C^I) (**SF6** in ESI†). **R$_2$–S–PS–COOH:** $M_{n(GPC)}$ = 3500 g mol^{-1}, M_w/M_n = 1.11. ^{1}H NMR(CDCl$_3$): $\delta_{(ppm)}$ = 7.43–6.00 (m, H^d), 4.70–4.35 (m, H^l), 3.42–3.18 (s, H$^{e'}$), 2.50–1.35 (m, H$^{f+g+h+k+j}$), 1.28–1.05 (s, H$_2^i$), 1.06–0.70 (m, H$_1^i$). ^{19}F NMR (CDCl$_3$): $\delta_{(ppm)}$ = −80.46 to −81.47, −119.85 to −121.05, −127.26 to −128.10 ppm. ^{13}C NMR (CDCl$_3$): δ(ppm) = 150.85–143.51 (C^{K+P}), 135.26–120.62 (C$^{L+R+T+V}$), 60.14–59.12 (C^Q), 53.36–35.54 (C$^{E+F+G+J}$), 35.07–20.98 (C$^{N+M+H+I}$) (**SF7** in ESI†). **R$_3$–S–PS–COOH:** $M_{n(GPC)}$ = 3800 g mol^{-1}, M_w/M_n = 1.12. ^{1}H NMR(CDCl^3): $\delta_{(ppm)}$ = 7.43–6.10 (m, H^d), 4.50–3.97 (s, H^l), 3.36–2.80 (m, H$^{e'}$), 2.70–1.28 (m, H$^{f+g+h+k+j+m+n}$), 1.28–1.01 (s, H$_2^i$), 1.00–0.80 (m, H$_1^i$). ^{19}F NMR (CDCl$_3$): $\delta_{(ppm)}$ = −80.90 to −81.68, −113.59 to −114.73, −121.20 to −124.45, −126.20 to −127.00 ppm. ^{13}C NMR (CDCl$_3$): δ(ppm) = 148.93–142.10 (C^{K+P}), 134.90–122.73 (C$^{L+V+W+Y}$), 52.36–36.43 (C$^{N+E+F+G+J}$), 34.59–20.20 (C$^{R+M+H+I}$) (**SF8** in ESI†).

Fabrication of α-fluorinated alkyl ester, ω-carboxyl telechelic PS porous films and microspheres

The fabrication of porous polymer films were carried out at 20 °C and 30 °C in static humid conditions, respectively, through casting different concentration of polymer solution in different solvents (CH$_2$Cl$_2$, CHCl$_3$ and CS$_2$) onto a clean glass substrate in a glass vessel with a cap. Saturated relative humidities (R. H.) in the glass vessel were achieved by adding saturated aqueous solutions of deionized water (R. H. = 95%) and methanol into the glass vessel, respectively.[58,63] After

complete evaporation of solvents, the porous polymer films and microspheres were formed on such glass slide and dried *in vacuo* at room temperature for characterization.

Polymers characterization

^{1}H NMR and ^{19}F NMR spectra of polymers were obtained on a Bruker AV 300 spectrometer (300 MHz) at room temperature with CDCl$_3$ as the solvent. The number molecular weight (M_n) and molecular weight distribution (M_w/M_n) of polymers were measured by a Waters gel permeation chromatography (GPC) system equipped with a Waters 1515 Isocratic HPLC pump, a Waters 2414 refractive index detector (RI), a Waters 2487 dual k absorbance detector (UV) and a set of Waters Styragel columns (HR3, HR4 and HR5, 7.8 × 300 mm). GPC measurements were carried out at 35 °C using tetrahydrofuran (THF) as eluent with a flow rate of 4.0 μL min^{-1}. The system was calibrated with polystyrene standards. The morphologies of fluoropolymer porous films were observed on a SEM (JSM 6390LV, JEOL, Japan) operated at 10 kV. The content of fluorine element on the surface of porous films were investigated by energy dispersive spectroscopy (EDS, Oxford, X-max 20). The hydrophobicity of such porous films were characterized *via* static water-droplet contact angles which were determined with a Power each JL2000L (Shanghai Zhongchen Digital Technic Facilities Ltd. Co.) contact-angle goniometer. A 1 μL droplet of deionized water was placed on the surface of a film, and the static contact angle was measured 30 s later. The average value of static water-droplet contact angles at five different positions on the porous film was provided. TEM images of microspheres were obtained by a JEM-1400 Transmission Electron Microscope (JEOL Ltd, Tokyo, Japan) operated at 100 kV.

Results and discussion

Synthesis of α-fluorinated alkyl ester, ω-carboxyl telechelic PS *via* combining aminolysis of RAFT-polystyrene and thiol–ene "click" reaction simultaneously

The synthetic procedure of α,ω-telechelic PS was illustrated in Scheme 1. According to our previously reported, the **R$_1$–S–PS–COOH** was synthesized *via* one-pot procedure using TFEA as ene-bearing compound under photoinitiation in the presence of DMPA.[29] The chain structure of the purified **R$_1$–S–PS–COOH** was confirmed by UV-vis, ^{1}H NMR, ^{13}C NMR and ^{19}F NMR spectra. The disappearance of C=S band at ~315 nm in UV-vis spectrum indicated the removal of thiocarbonylthio moiety (**SF2** *vs.* **SF1** of **PS-CTA** in ESI†). Both of the singlets at 5.03–4.60 and 3.25 ppm assigned to the methine proton (e) (–SC(=S)S–CH(Ph)–) and methylene protons (c) next to thiocarbonylthio of **PS-CTA** were disappeared (Fig. 1(A)), while new singlets at 4.40 and 3.30 ppm assigned to methylene protons next to –CF$_3$ moiety and methine proton (–CH$_2$–S–CH(Ph)–) present. The ^{13}C NMR spectrum of **R$_1$–S–PS–COOH** (**SF6**) also show new characteristic peaks and the disappearance of peaks belonging to thiocarbonylthio moiety of **PS-CTA** (**SF5**). The incorporation of –CF$_3$ moiety was also confirmed by three singlets at −73.67, −73.70 and −73.72 ppm in ^{19}F NMR spectrum (Fig. 2(A)). The M_ns of polymers before and after one-pot
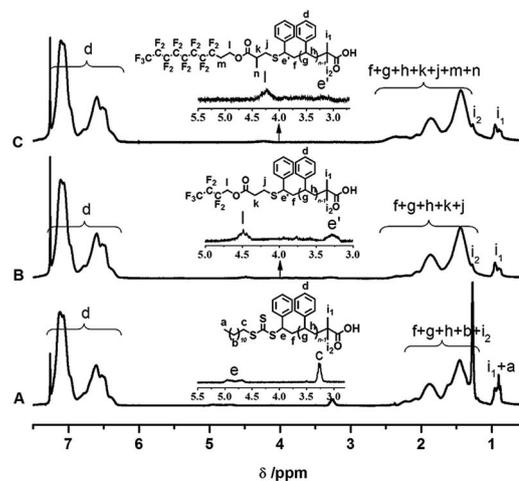

Fig. 1 ^{1}H NMR spectra of (A) PS-CTA, (B) R$_2$–S–PS–COOH and (C) R$_3$–S–PS–COOH.

procedure increased from 3200 to 3400 g mol^{-1} which also confirmed the transformation of terminal moieties.

R$_2$–S–PS–COOH can be prepared in one-pot procedure using HFBA as ene-bearing compound under photoinitiation in the presence of DMPA. The chain structure of such purified polymer was confirmed by UV-vis, ^{1}H NMR, ^{13}C NMR and ^{19}F NMR spectra. The disappearance of C=S band at ~315 nm in UV-vis spectrum indicated the removal of thiocarbonylthio moiety (**SF3** in ESI†). As shown in Fig. 1(B), compared with **PS-CTA**, new singlets at 4.7–4.35 and 3.42–3.18 ppm assigned to methylene protons (l) next to –O–CH$_2$–CF$_2$– moiety and methine proton (e′) (–CH$_2$–S–CH(Ph)–) present. In the ^{13}C NMR spectrum of **R$_2$–S–PS–COOH** (**SF7**), the disappearance of peaks belonging to thiocarbonylthio moiety of **PS-CTA** (**SF5**) while the presence of new characteristic peaks assigned to fluorinated moiety also indicated the successful transformation of the terminal moieties. The incorporation of –CF$_3$, –CF$_2$–CF$_3$, –CH$_2$–CF$_2$– moiety was also confirmed by singlets at −80.46 to −81.47, −127.26 to −128, −119.85 to −121.05 ppm in ^{19}F NMR spectrum,
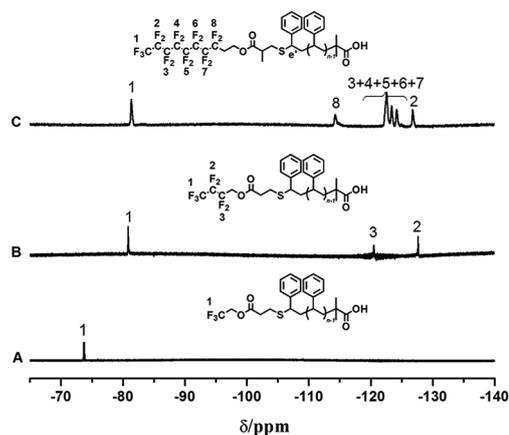

Fig. 2 ^{19}F NMR spectra of (A) R$_1$–S–PS–COOH, (B) R$_2$–S–PS–COOH, and (C) R$_3$–S–PS–COOH.

respectively (Fig. 2(B)).[65] The M_n of polymers before and after one-pot procedure increased from 3200 to 3500 g mol^{-1} indicating the transformation of thiocarbonylthio to fluorinated moiety.

Unexpectedly, **R$_3$–S–PS–COOH** can not be prepared in one-pot procedure using HDFDM as ene-bearing compound *via* one-pot procedure described above. Interestingly, a tandem strategy was successfully employed for the synthesis of **R$_3$–S–PS–COOH**. The synthetic procedure of **R$_3$–S–PS–COOH** was illustrated in Scheme 1. The detail research on the significant difference between such two synthetic methods is under way. The chain structure of the purified **R$_3$–S–PS–COOH** was confirmed by UV-vis, ^{1}H NMR, ^{13}C NMR and ^{19}F NMR spectra. The disappearance of C=S band at ~315 nm in UV-vis spectrum indicated the removal of thiocarbonylthio moiety (**SF4** in ESI†). As shown in Fig. 1(C), compared with the spectrum of **PS–CTA**, new singlets at 4.50–3.97 and 3.36–2.80 ppm assigned to methylene protons (l) next to –O–CH$_2$– moiety and methine proton (e') (–CH$_2$–S–CH(Ph)–) present. The new characteristic peaks in ^{13}C NMR spectrum of **R$_3$–S–PS–COOH** (**SF8**) also confirmed its chain structure. The incorporation of –CF$_3$, –CF$_2$–CF$_3$, –(CF$_2$)$_5$–, –CH$_2$–CF$_2$– moiety was also confirmed by singlets at −80.90 to −81.68, −126.20 to −127.00, −121.20 to −124.45, −113.59 to −114.73 ppm in ^{19}F NMR spectrum, respectively (Fig. 2(C)).[34,66] The M_n of polymers before and after aminolysis/thiol–ene click reaction increased from 3200 to 3800 g mol^{-1} indicating the replacement of thiocarbonylthio by fluorinated moiety.

The morphology and hydrophobicity of α-fluorinated alkyl ester, ω-carboxyl telechelic PS porous films and microspheres by a static BF process

As has been reported, amphiphilic polymers are believed to be good candidates to form highly ordered porous films by the breath-figure (BF) process because of their high segment density which could effectively stabilize water droplets in BF method.[42] Nevertheless, A variety of parameters would influence the formation of highly ordered porous films such as relative humidity (R. H.), temperature, solvent, the architecture and component of polymers, polymer concentration and so on.[44,45,67] In this paper, some critical factors such as solvent, temperature, the architecture and concentration of polymer which influence on the morphology of polymer porous film in BF process were investigated.

As reported in the literature,[58] the relative humidity (R. H.) of 95% facilitated the formation of water droplets, and more water droplets sinking into the solution surface and being caught by the terminal carboxyl group of **PS–COOH**, would result in ordered porous films on the substrate after the water droplets and solvent evaporated completely. Herein, the R. H. of 95% were employed in all cases of static BF process for fabricating porous films. Firstly, dichloro methane (CH$_2$Cl$_2$), chloroform (CHCl$_3$) and carbon disulfide (CS$_2$) were used as solvent, respectively, in the static BF procedure for fabricating **R$_1$–S–PS–COOH** porous films in the concentration of 20 mg mL^{-1} at 20 °C and R. H. of 95%. SEM images of the obtained polymer porous
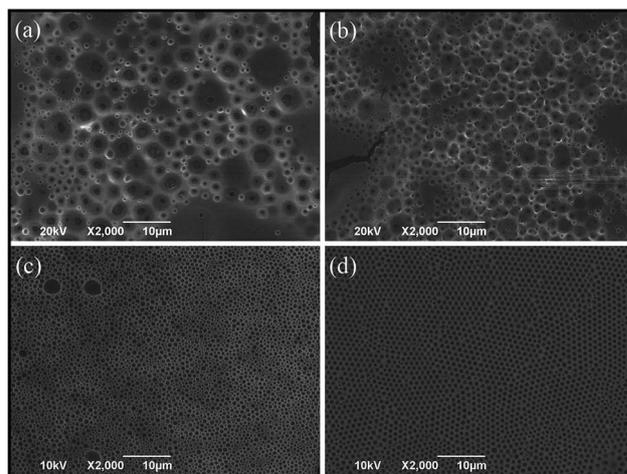

Fig. 3 SEM images of **R$_1$–S–PS–COOH** porous films fabricated *via* a static breath-figure process under R. H. of 95% at 20 °C with polymer concentration of 20 mg mL^{-1} in different solvents: (a) CH$_2$Cl$_2$, (b) CHCl$_3$, (c) CS$_2$. (d) CS$_2$, at 30 °C.

films are shown in Fig. 3. The **R$_1$–S–PS–COOH** porous films prepared in CS$_2$ (Fig. 3(c)) were more regular than those prepared in CH$_2$Cl$_2$ (Fig. 3(a)) and CHCl$_3$ (Fig. 3(b)) solutions. It is ascribed that CS$_2$ has a lower water solubility and higher surface tension. Additionally, CS$_2$ also has a low miscibility and a high interfacial tension with water. Therefore, during the process, CS$_2$ has a higher volatility leading to the lower surface temperature, which can quickly condense water droplets. Hence, CS$_2$ is the best solvent for forming porous films in this case. The different fabrication temperature of 30 °C was also employed in the static BF process. As shown in Fig. 3, the polymer porous film with higher regularity was achieved at 30 °C (Fig. 3(d)) comparing with that at 20 °C (Fig. 3(c)). The possible explanation is that, as we known, the temperature has effect on not only the evaporation of the solvent, but also the partial pressure of the water vapor which provides the water source and forms the droplet on the film, so it is difficult to form highly regular microstructured polymer film if the ambient temperature is too low to make the water vapor condense. Additionally, the higher the temperature, the faster the evaporation of the solvent and the higher partial pressure of the water vapor, resulting the bigger and faster temperature drop while the evaporation of the solvent and thus the more moist ambient condition provide sufficient water to form bigger droplet which finally yielded the bigger pore size.

Being one of significant factors, polymer concentration also influences the formation and morphology of polymer porous films. Hence, the **R$_1$–S–PS–COOH** porous films were fabricated at 30 °C and under R. H. of 95% in CS$_2$ with different concentration of 10, 20, 30 and 40 mg mL^{-1}, respectively. As observed by SEM in Fig. 4, the formation of disordered porous film was probably due to the combined effects of lower solution viscosity and lower concentration of –COOH group in 10 mg mL^{-1} polymer solution, which can not inhibit the coalescence of water droplets efficiently, resulting in larger pores (1.60 μm) and
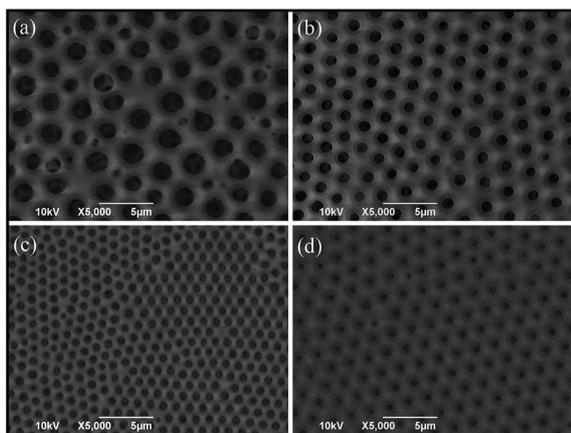
Fig. 4   SEM images of R₁−S−PS−COOH porous films fabricated under R. H. of 95% at 30 °C with CS₂ as solvent at different polymer concentration: (a) 10 mg mL⁻¹, (b) 20 mg mL⁻¹, (c) 30 mg mL⁻¹, (d) 40 mg mL⁻¹.

less regularity. With the concentration rising to 20, 30 and 40 mg mL⁻¹, the average pore sizes of the obtained films decreased from 0.98 μm to 0.69 μm and 0.58 μm, respectively. The arrangement of pores on the surface of the obtained porous films became more uniform and the average pore sizes were decreased. Such tendency can be explained by a larger surface area of the water droplets stabilized by increasing polymer concentration before the precipitation of the polymers. Because of the architecture of polymer influencing on the morphology of polymer porous film, the porous films of PS-CTA, R₂–S–PS–COOH and R₃–S–PS–COOH were also investigated in BF process. We found that the porous films of PS-CTA, R₁–S–PS–COOH, R₂–S–PS–COOH, R₃–S–PS–COOH have the same average pore size of ca. 1.00 μm via the static BF process under R. H. of 95% with CS₂ as solvent (20 mg mL⁻¹) (shown in Fig. 5). Such tendency may be explained by lower content of fluoric group and similar molecular weight in polymers, which can not inhibit significant change.
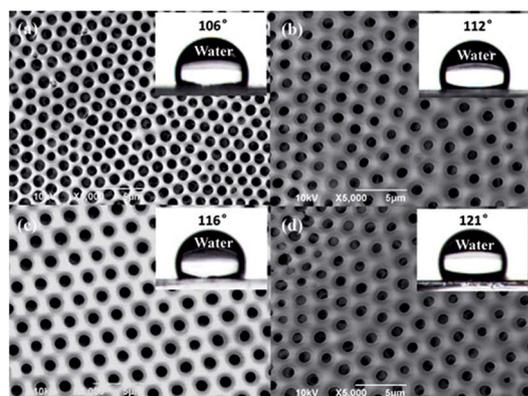

Fig. 5   SEM images of different α-fluorinated alkyl ester, ω-carboxyl-telechelic PS porous films fabricated under R. H. of 95% with CS₂ as solvent: (a) PS-CTA, (b) R₁–S–PS–COOH, (c) R₂–S–PS–COOH, (d) R₃–S–PS–COOH.

Hydrophobic and super-hydrophobic/ultra-hydrophobic materials were defined as materials with surfaces which have water-droplet contact angles more than 90° and 150°, respectively. In general, both the surface chemistry and the surface roughness affect hydrophobicity. Fluoropolymers are known to have very excellent hydrophobicity.[33] In order to investigate the influence of fluorine element content on the hydrophobicity of porous films, we selected the porous films of PS-CTA and three α-fluorinated alkyl ester, ω-carboxyl telechelic PS with the same average pore size of ca. 1.00 μm. The hydrophobicity of the obtained polymer porous film was characterized by contact angle of water-droplet on its surface. As observed by SEM in Fig. 5, the porous film of PS-CTA without any fluorine units showed a water-droplet contact angle (WCA) of 106° ± 0.4° (Fig. 5(a)). With the increase of fluorine element content determined by EDS from 1.04 wt% (R₁–S–PS–COOH) to, 1.64 wt% (R₂–S–PS–COOH) and 2.97 wt% (R₃–S–PS–COOH), the static water-droplet contact angles increased from 112° to 116° and 121° ± 0.4°, respectively. This indicated that the fluoromethylene (–CF₂) and terminal fluoromethyl (–CF₃) groups of the pendant fluoroalkyl chain tend to localize at the air–polymer interface, resulting in fluoroacrylate content in the polymers lowered the surface free energy of the polymer and conversely increased its WCA.[34–36] Therefore, PS with fluoroalkyl pendant group showed higher WCA than that of PS-CTA. Furthermore, with increasing fluoroalkyl pendant group, the WCA would increase.[31]

Usually, the static BF process was carried out in an aqueous vapor atmosphere, porous films were fabricated via the condensed water droplets from a moist environment on the solution surface by rapid evaporation of organic solvent, acting as templates to precipitate polymers. However, when the water environment in the chamber was replaced with methanol, microspheres rather than porous films were formed. In addition the polymer microspheres were widely used in separation, catalysis carriers, drug delivery and so on directly or after surface functionalization.[57–62] Therefore, in this article the microspheres of R₁–S–PS–COOH, R₂–S–PS–COOH and R₃–S–PS–COOH were successfully fabricated at 30 °C with CS₂ as solvent (20 mg mL⁻¹) casting onto the glass slides in a chamber filled with methanol vapor. The shape and average diameter of the particles have been analyzed by SEM and TEM as shown in Fig. 6. The average sizes of polymer particles were ranging from 0.30 to 0.65 and 0.39 μm. The morphology of R₁–S–PS–COOH particle was well-defined, spherical and uniform (Fig. 6(a)). However, the morphology of R₂–S–PS–COOH and R₃–S–PS–COOH particle was not well-defined, spherical and uniform (Fig. 6(b) and (d)). The driving force for the particles formation of the amphiphilic polymer probably involved strong repulsion between the highly hydrophobic –CF₃ and hydrophilic –COOH tails. In the initial CS₂ solution, the polymer molecules remain well dispersed. When MeOH liquid droplets condense on the cooling surface of α-fluorinated alkyl ester, ω-carboxyl-telechelic PS/CS₂ solution, it dissolved in the polymer solution, shrinked to form dispersed micro-droplets together, concurrently rapid evaporation of organic solvent, the hydrophilic –COOH tails become even more extended, while the hydrophobic –CF₃ tails collapsed by phase inversion to minimize the surface
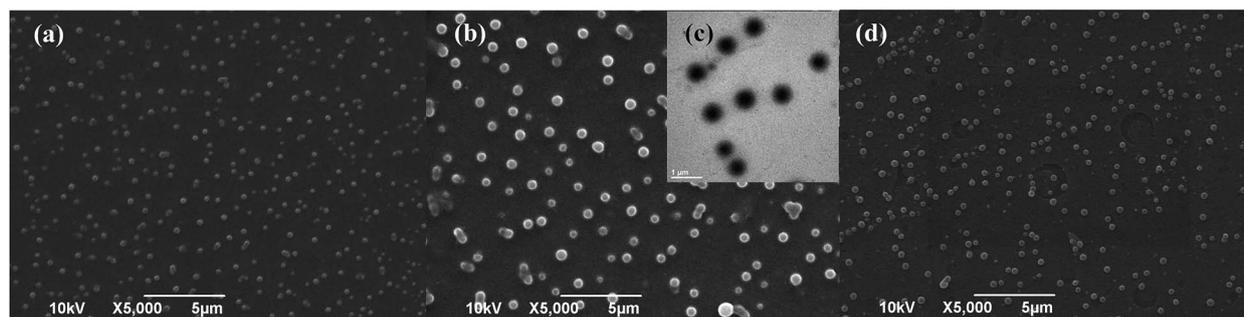
Fig. 6 Different α-fluorinated alkyl ester, ω-carboxyl-telechelic PS porous films fabricated under methanol at 30 °C with CS_2 as solvent (20 mg mL^{-1}): (a) SEM of R_1–S–PS–COOH; (b) R_2–S–PS–COOH; (c) TEM of R_2–S–PS–COOH; (d)R_3–S–PS–COOH.

area. Because of the surface tension effect and the interfacial energy of the micro-droplets, microspheres films were formed in all cases. The formation of disordered particles was probably due to the combined effects of lower solution viscosity, environmental factors and lower concentration of –COOH group in polymer solution, which cannot inhibit the coalescence of droplets efficiently, resulting in larger microspheres (about 0.65 μm) and less regularity.[58] The possible explanation for such phenomenon is under work. TEM images of R_2–S–PS–COOH were shown that α-fluorinated alkyl ester, ω-carboxyl-telechelic PS particles were well-dispersed without aggregation (Fig. 6(c)). The important feature of the TEM images of the fluoropolymer was that it possibly has core–shell morphology.[68]

Conclusions

Three α-fluorinated alkyl ester, ω-carboxyl telechelic polystyrenes were successfully synthesized *via* combining aminolysis of RAFT-polystyrene and thiol–ene "click" reaction under incandescent-lamp irradiation with photoinitiator. Their porous films with good regularity were fabricated *via* a static breath-figure process under R. H. of 95% at 30 °C in CS_2 solution with polymer concentration of 20–40 mg mL^{-1}. With the change of fluorinated chain end from –CF_3 to –C_3F_7 and –C_8F_{17}, R_1–S–PS–COOH, R_2–S–PS–COOH and R_3–S–PS–COOH ordered porous films with average pore size of *ca.* 1.00 μm displayed good hydrophobicity with static water-droplet contact angles of 112°, 116° and 121°, respectively. Interestingly, R_1–S–PS–COOH, R_2–S–PS–COOH microspheres with the average diameters 0.30 μm, 0.65 and 0.39 μm can be fabricated using methanol instead of water as vapor atmosphere in the glass vessel, respectively. TEM images of R_2–S–PS–COOH showed that α-fluorinated alkyl ester, ω-carboxyl-telechelic PS particles were dispersed, and no aggregation. The important feature of the TEM images of the fluoropolymer was that it has core–shell morphology. The possible applications of such microporous film and microspheres are under investigation.

Acknowledgements

Notes and references

1 J. Kima, S. S. Kim, K. H. Kim, Y. H. Jin, S. M. Hong, S. S. Hwang, B. G. Cho, D. Y. Shin and S. S. Im, *Polymer*, 2004, **45**, 3527–3533.

2 Y. Liu and C. Y. Pan, *Eur. Polym. J.*, 1998, **34**, 621–624.

3 X. D. Lou, C. Detrembleur and R. Jérôme, *Macromolecules*, 2002, **35**, 1190–1195.

4 J. Liu, C. Y. Hong and C. Y. Pan, *Polymer*, 2004, **45**, 4413–4421.

5 P. G. Liu, H. Y. Ding, J. N. Liu and X. S. Yi, *Eur. Polym. J.*, 2002, **38**, 1783–1789.

6 C. W. Bielawski, J. M. Jethmalani and R. H. Grubbs, *Polymer*, 2003, **44**, 3721–3726.

7 N. Hadjichristidis, S. Pispas and M. Pitsikalis, *Prog. Polym. Sci.*, 1999, **24**, 875–915.

8 S. Kéki, M. Nagy, G. Deák, A. Lévai and M. Zsuga, *J. Polym. Sci., Part A: Polym. Chem.*, 2002, **40**, 3974–3986.

9 M. A. Peters, A. M. Belu, R. W. Linton, L. Dupray, T. J. Meyer and J. M. DeSimone, *J. Am. Chem. Soc.*, 1995, **117**, 3380–3388.

10 R. P. Quirk and G. M. Lizárraga, *Macromolecules*, 1998, **31**, 3424–3430.

11 A. Hirao, H. Nagahama, T. Ishizone and S. Nakahama, *Macromolecules*, 1993, **26**, 2145–2150.

12 A. Hirao, M. Tohoyama and S. Nakahama, *Macromolecules*, 1997, **30**, 3484–3489.

13 S. Nayak, H. Verma and T. Kannan, *Colloid Polym. Sci.*, 2010, **288**, 181–188.

14 O. Altintas, T. Rudolph and C. Barner-Kowollik, *J. Polym. Sci., Part A: Polym. Chem.*, 2011, **49**, 2566–2576.

15 D. J. Siegwart, J. K. Oh, H. Gao, S. A. Bencherif, F. Perineau, A. K. Bohaty, J. O. Hollinger and K. Matyjaszewski, *Macromol. Chem. Phys.*, 2008, **209**, 2179–2193.

16 B. Aydogan and Y. Yagci, *Turk. J. Chem.*, 2007, **31**(1), 1–10.

17 D. L. Patton, M. Mullings, T. Fulghum and R. C. Advincula, *Macromolecules*, 2005, **38**, 8597–8602.

18 V. Lima, X. L. Jiang, J. Brokken-Zijp, P. J. Schoenmakers, B. Klumperman and R. V. D. Linde, *J. Polym. Sci., Part A: Polym. Chem.*, 2005, **43**, 959–973.

19 G. Moad, Y. K. Chong, A. Postma, E. Rizzardo and S. H. Thang, *Polymer*, 2005, **46**, 8458–8468.

20 F. Segui, X. P. Qiu and F. M. Winnik, *J. Polym. Sci., Part A: Polym. Chem.*, 2008, **46**, 314–316.

21 C. Boyer, J. Q. Liu, V. Bulmus, T. P. Davis, C. Barner-Kowollik and M. H. Stenzel, *Macromolecules*, 2008, **41**, 5641–5650.

22 C. Boyer, A. Granville, T. P. Davis and V. Bulmus, *J. Polym. Sci., Part A: Polym. Chem.*, 2009, **47**, 3773–3794.

23 N. A. Cortez-Lemus, R. Salgado-Rodriguez and A. Licea-Claverie, *J. Polym. Sci., Part A: Polym. Chem.*, 2010, **48**, 3033–3051.

24 K. Dan and S. Ghosh, *Angew. Chem., Int. Ed.*, 2013, **52**, 7300–7305.

25 X. P. Qiu and F. M. Winnik, *Macromol. Rapid Commun.*, 2006, **27**, 1648–1653.

26 M. J. Stanford and A. P. Dove, *Macromolecules*, 2009, **42**, 141–147.

27 J. W. Chan, B. Yu, C. E. Hoyle and A. B. Lowe, *Polymer*, 2009, **50**, 3158–3168.

28 J. W. Chan, B. Yu, C. E. Hoyle and A. B. Lowe, *Chem. Commun.*, 2008, 4959–4961.

29 S. S. Zhang, K. Cui, J. Huang, Q. L. Zhao, S. K. Cao and Z. Ma, *RSC Adv.*, 2015, **5**, 44571–44577.

30 A. Bruno, *Macromolecules*, 2010, **43**, 10163–10184.

31 K. Li, P. P. Wu and Z. W. Han, *Polymer*, 2002, **43**, 4079–4086.

32 K. Honda, M. i. Morita, H. i. Otsuka and A. Takahara, *Macromolecules*, 2005, **38**, 5699–5705.

33 *Fluoropolymers*, ed. G. Hougham, P. E. Cassidy, K. Johns and T. Davidson, Kluwer Academic Publishers, New York, 1999, vol. I and II.

34 S. Borkar, K. Jankova, H. W. Siesier and S. Hvilsted, *Macromolecules*, 2004, **37**, 788–794.

35 S. Hvilsted, *Polym. Int.*, 2014, **63**, 814–823.

36 B. P. Koiry, H. A. Klok and N. K. Singha, *J. Fluorine Chem.*, 2014, **165**, 109–115.

37 H. Yamaguchi, M. Kikuchi, M. Kobayashi, H. Ogawa, H. Masunaga, O. Sakata and A. Takahara, *Macromolecules*, 2012, **45**, 1509–1516.

38 B. Guyot, B. Ameduri and B. Boutevin, *J. Fluorine Chem.*, 1995, **74**, 233–240.

39 L. J. Chen, H. X. Shi, H. K. Wu and J. P. Xiang, *J. Fluorine Chem.*, 2010, **131**, 731–737.

40 M. Robinson and J. K. Kochi, *Macromolecules*, 1983, **16**, 526–532.

41 Z. H. Mao, K. Vakhshouri, C. Jaye, D. A. Fischer, R. Fernando, D. M. DeLongchamp, E. D. Gomez and G. Sauvé, *Macromolecules*, 2013, **46**, 103–112.

42 P. Escalé, L. Rubatat, L. Billon and M. Save, *Eur. Polym. J.*, 2012, **48**, 1001–1025.

43 O. Karthaus, N. Maruyama, X. Cieren, M. Shimomura, H. Hasegawa and T. Hashimoto, *Langmuir*, 2000, **16**, 6071–6076.

44 J. L. Gong, L. C. Sun, Y. W. Zhong, C. Y. Ma, L. Li, S. Y. Xie and V. Svrcek, *Nanoscale*, 2012, **4**, 278–283.

45 U. Heiko and F. Bunz, *Adv. Mater.*, 2006, **18**, 973–989.

46 H. Bai, C. Du, A. J. Zhang and L. Li, *Angew. Chem., Int. Ed.*, 2013, **52**, 12240–12255.

47 M. Herandez-Guerrero and M. H. Stenzel, *Polym. Chem.*, 2012, **3**, 563–577.

48 L. Li, C. K. Chen, J. Li, A. J. Zhang, X. Y. Liu, B. Xu, S. B. Gao, G. H. Jin and Z. Ma, *J. Mater. Chem.*, 2009, **19**, 2789–2796.

49 J. Li, Q. L. Zhao, J. Z. Chen, L. Li, J. Huang, Z. Ma and Y. W. Zhong, *Polym. Chem.*, 2010, **1**, 164–167.

50 L. Li, J. Li, Y. W. Zhong, C. K. Chen, Y. Ben, J. L. Gong and Z. Ma, *J. Mater. Chem.*, 2010, **20**, 5446–5453.

51 L. Li, Y. W. Zhong, J. L. Gong, J. Li, C. K. Chen, B. Zeng and Z. Ma, *Soft Matter*, 2011, **7**, 546–552.

52 T. Kawano, Y. Nakamichi, S. Fujinami, K. Nakajima, H. Yabu and M. Shimomura, *Biomacromolecules*, 2013, **14**, 1208–1213.

53 L. S. Wan, J. W. Li, B. B. Ke and Z. K. Xu, *J. Am. Chem. Soc.*, 2012, **134**, 95–98.

54 H. Yabu, M. Takebayashi, M. Tanaka and M. Shimomura, *Langmuir*, 2005, **21**, 3235–3237.

55 L. S. Wan, Q. L. Li, P. C. Chen and Z. K. Xu, *Chem. Commun.*, 2012, **48**, 4417–4419.

56 C. Du, A. J. Zhang, H. Bai and L. Li, *ACS Macro Lett.*, 2013, **2**, 27–30.

57 X. P. Xiong, W. W. Zou, Z. J. Yu, J. J. Duan, X. J. Liu, S. H. Fan and H. Zhou, *Macromolecules*, 2009, **42**, 9351–9356.

58 J. P. Gao, W. Wu, L. Rong, G. L. Mao, Y. N. Ning, Q. L. Zhao, J. Huang and Z. Ma, *Eur. Polym. J.*, 2014, **59**, 171–179.

59 J. Y. Ding, A. J. Zhang, H. Bai, L. Li, J. Lia and Z. Ma, *Soft Matter*, 2013, **9**, 506–514.

60 H. Kawaguchi, *Prog. Polym. Sci.*, 2000, **25**, 1171–1210.

61 S. Freiberg and X. X. Zhu, *Int. J. Pharm.*, 2004, **282**, 1–18.

62 A. S. Goldmann, L. Barner, M. Kaupp, A. P. Vogt and C. Barner-Kowollik, *Prog. Polym. Sci.*, 2012, **37**, 975–984.

63 Y. Xue, H. C. Lu, Q. L. Zhao, J. Huang, S. G. Xu, S. K. Cao and Z. Ma, *Polym. Chem.*, 2013, **4**, 307–312.

64 A. Munoz-Bonilla, E. Ibarboure, E. Papon and J. Rodriguez-Hernandez, *Langmuir*, 2009, **25**(11), 6493–6499.

65 S. B. Chen and W. H. Binder, *Polym. Chem.*, 2015, **6**, 448–458.

66 K. Skrabania, H. v. Berlepsch, C. Bottcher and A. Laschewsky, *Macromolecules*, 2010, **43**, 271–281.

67 M. H. Stenzel, *Aust. J. Chem.*, 2002, **55**, 239–243.

68 A. Chakrabarty and N. K. Singha, *J. Colloid Interface Sci.*, 2013, **408**, 66–74.